*International Tables for Crystallography* (2006). Vol. F, Section 9.1.10, pp. 189–190.



safer to use a wavelength which is 0.001–0.002 Å shorter (or use an energy 10–20 eV higher) than the edge recorded from the standard. When using anomalous scatterers displaying large white lines within their spectra, the wavelength should be accurately adjusted on the basis of the spectrum measured from the actual sample.

For collecting data without an anomalous signal, there are no strict requirements concerning the wavelength. The maximum intensity provided by the beamline depends on the energy of particles in the synchrotron storage ring and on the beamline optics. Typically, wavelengths around 1 Å or shorter are used at most synchrotrons, assuring high beam intensity and low absorption of X-rays by the sample and air, thus reducing the radiation damage of the crystal. This is of particular importance at the very bright beamlines at third-generation synchrotrons. To diminish the effect of air absorption further, it is possible to fill the space between the crystal and the detector with helium. Short wavelengths are advantageous for collecting high-resolution data, since the diffraction angles are smaller and there is no need to use a very short CTDD. The effect of profile elongation owing to the oblique incidence of diffracted X-ray beams on the detector is then smaller, and the blind region is narrower.

### 9.1.10. Lysozyme as an example

Tetragonal hen egg-white lysozyme (Chapter 26.1 and Blake *et al.*, 1967), crystallizing in the space group $P4_32_12$ with cell dimensions $a = b = 78.6$ and $c = 37.2$ Å, is used here as a model system to illustrate some of the points made above, based on Dauter (1999). The example involves a set of two consecutive blocks of images with a crystal-to-detector distance of 243 mm, a wavelength of 0.92 Å, a resolution of 2.7 Å, an oscillation range of 1.5° and a crystal mosaicity around 0.5°. These images are shown in Fig. 9.1.10.1(*a–f*).

The first four images, (*a–d*), were exposed with the tetragonal fourfold *c* axis lying approximately along the direction of the beam. On these images, the reflections within each lune are arranged in a square grid, reflecting the tetragonal symmetry with $a = b$. The squares are oriented with their diagonals in the horizontal and vertical directions of the image, as the crystal was mounted with its [110] direction along the spindle rotation axis. Indeed, at the end of image (*a*) and the start of image (*b*), the *c* axis lay almost perfectly along the beam, and the zero-layer lune almost disappears behind the beam-stop shadow, since the corresponding (*hk*0) plane in reciprocal space is tangential to the Ewald sphere at the origin of the reciprocal lattice.

The lunes are widely spaced with clear gaps between them, because the third cell dimension, *c*, which is perpendicular to the detector plane, is relatively short, 37.2 Å. Images (*e–f*), exposed at an angle on the rotation spindle roughly 90° away from (*a–d*), have a quite different appearance, despite the rotation range per image being the same. Each lune is less densely populated by reflections, but the number of lunes is larger and the gaps between them much smaller. This arises from the lunes now being parallel to the (*hhl*) family of planes, as the $[1\bar{1}0]$ vector is now parallel to the beam. The interplanar spacing within this family is less than for those on

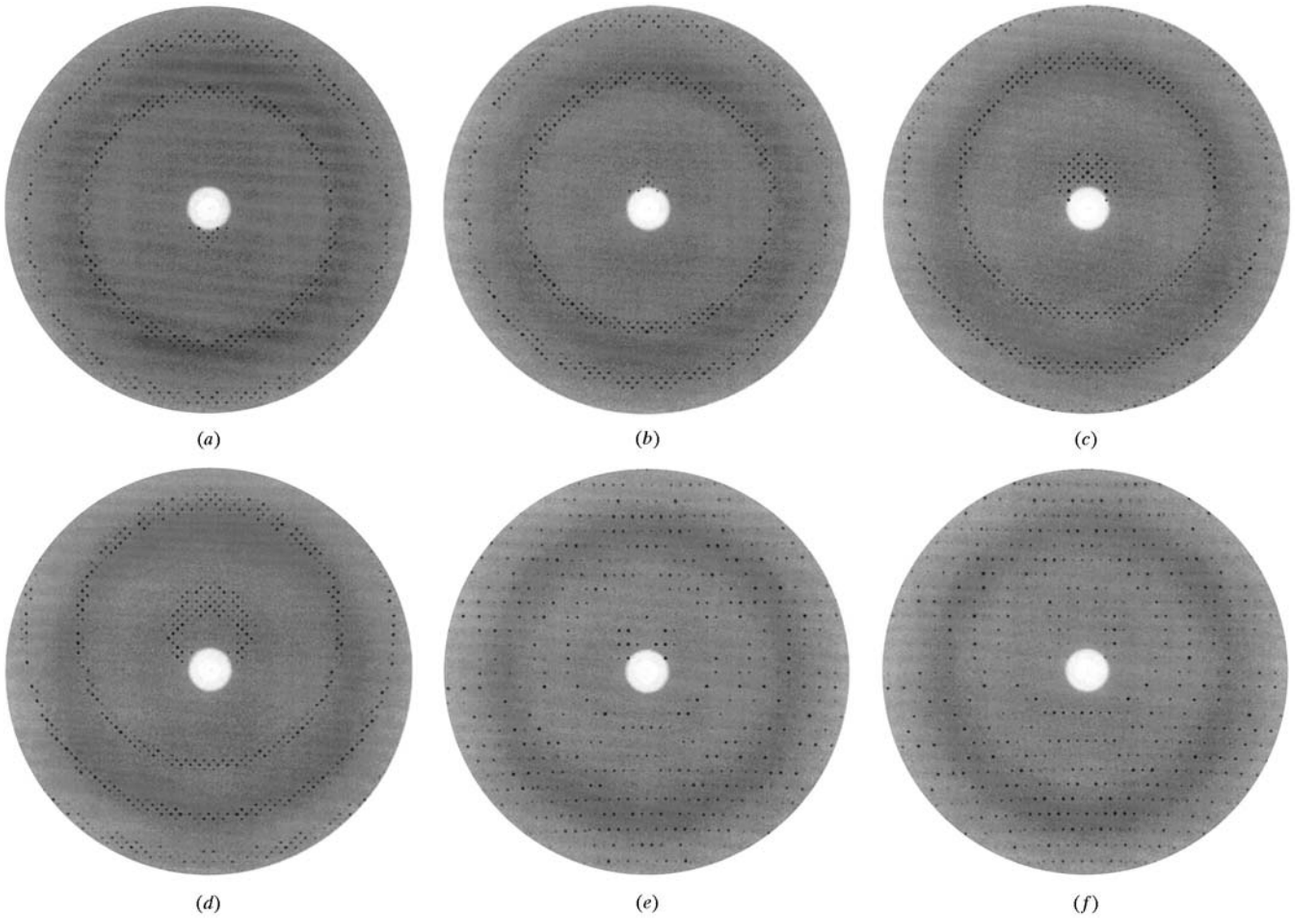


Fig. 9.1.10.1. Images recorded from a crystal of lysozyme. (*a–d*) Four consecutive exposures with the crystal fourfold axis parallel to the X-ray beam. (*e–f*) Two successive exposures 90° away, when the fourfold axis lies vertically in the plane of the image. The crystal [110] direction is parallel to the rotation axis, horizontal in the plane of the images.

images (*a*–*d*), hence at high resolution, close to the edge of the detector window, the lunes overlap on images (*e*–*f*). The reflections, however, do not overlap, as the crystal orientation is diagonal; the lunes are sparsely populated, with large separation between adjacent spots, so the reflections on successive lunes fit between one another. It should be noted that the density of reflections in different regions of the reciprocal lattice is constant, and that the total number of reflections recorded on an image depends only on the rotation range, not on the crystal orientation.

The zero-layer lune containing reflections with indices *hk*0 is especially evident on exposures (*c*–*d*) directly above the centre of the image. With such a lune close to the centre, the reciprocal lattice shows minimal distortion owing to its projection onto the detector plane, and the lune appears as a 'pseudoprecession' pattern. The systematic absence of every second reflection, with odd index, along the *h*00 and 0*k*0 lines indicates the presence of twofold screw axes of symmetry along the crystal axes *a* and *b*. Images (*e*–*f*), 90° away, have the *hhl* lune at the centre and, although it is less well separated from higher lunes, the presence of a fourfold screw axis along **c** is confirmed by the presence of only every fourth reflection on the 00*l* line. This allows the identification of the space group as $P4_12_12$ or its enantiomorph, $P4_32_12$. In general, the positions of the reflections define only the Bravais lattice, and it is symmetry of the intensity pattern which reflects the point group. Thus, further confirmation that the symmetry belongs to point group *P*422 rather than *P*4 comes from the symmetric relation of the intensity distribution on either side of each lune in images (*a*–*d*). This is equivalent to the earlier use of precession photography for space-group elucidation.

Close inspection shows that the reflections at the edges of the lune are also present on the adjacent image. The rotation range was 1.5°, and the mosaicity was estimated at 0.5°, and thus about one-sixth of the reflections are partially recorded at each edge of the lune, giving one-third partially recorded terms in total. The lack of sharpness at the edge of the lunes confirms a substantial level of mosaicity.

## 9.1.11. Rotation method: qualitative factors

### 9.1.11.1. *Inspection of reflection profiles*

Reflection profiles should be checked on the first recorded images. Very often a quick inspection of the profiles can disqualify a bad crystal without further loss of time. The profiles should have a single maximum and smooth shoulders. If the crystal shape is irregular, it may be reflected in the spot profile. Profiles should not have double maxima or be substantially elongated or smeared out, which usually arises from crystal splitting. The profiles should certainly be inspected if initial autoindexing of the diffraction pattern is unsuccessful.

Even if the spot profiles appear to be regular on the first image, it is good practice to inspect a second image at a substantially different $\varphi$ rotation angle, preferably 90° away, since crystal splitting may have a similar effect on the appearance of the lunes and profiles as does high mosaicity on a single image (Section 9.1.6.3). High mosaicity and splitting (often incorrectly referred to as twinning) must not be confused. If two parts of a split crystal are slightly rotated with respect to one another around a certain axis, the diffraction patterns will look different depending on the orientation. When such an axis is perpendicular to the detector plane, the spots will be doubled or smeared out. When the axis is parallel to the detector plane, the profiles resulting from the two parts of the crystal will overlap almost perfectly, but the lunes will be broadened, similar to the effect of high mosaicity.

After indexing the diffraction pattern, the integration profiles should be matched with the size and shape of the diffraction spots. The spots should not extend into the area defined as background. Selection of integration profiles that are too small will lead to incorrect integration of intensities. In contrast, if the profile areas are too large then the standard uncertainties will be wrongly estimated.

### 9.1.11.2. *Exposure time*

According to the principles of counting statistics, the longer the exposure, the better the signal in the data. The standard uncertainty of the measurement is equal to the square root of the number of counts, and the signal-to-noise ratio increases with the accumulated counts. In practice there are limitations to this rule.

The dynamic range and saturation limit of the detector is one limiting factor. It may be impossible to measure adequately the strongest as well as the weakest reflection simultaneously, since their intensities differ by several orders of magnitude. If the exposure time is long enough to record the weakest intensities, then in general at low resolution the most intense reflections may saturate some pixels within their profile on the detector. Such reflections are termed 'overloads' and this problem will be addressed in Section 9.1.11.3.

Exposure time can be limited by the total time available for the experiment. This is often a particularly acute problem for synchrotron-data collection, with high oversubscription of beam-lines. The decisions concerning exposure time depend on the expected application of the data, since different applications have different requirements, as addressed in Section 9.1.13. Within the given time constraints, the first priority should be data completeness, even at the expense of underexposure. In this context it is useful to recall that to increase the statistical signal-to-noise ratio by a factor of two, it is necessary to prolong the exposure time by at least a factor of four.

### 9.1.11.3. *Overloads*

Some detectors, or their associated read-out systems, are limited in the number of counts they can accumulate in one pixel. The number recorded reaches a maximum number which cannot be further increased, *i.e.* the pixels can become saturated. This means that these pixels retain the same maximum value on longer exposure whilst other, non-saturated, pixels continue to accumulate counts. The intensity in saturated pixels will hence be underestimated compared to the others and any intensities estimated from profiles including such pixels will be biased towards low values. It is essential that pixels that are saturated are flagged and recognized by the processing software. There are several ways to deal with the problem of saturation.

(1) Reject all reflections that contain saturated pixels. These will tend to be at low resolution. If more than a very few are rejected, this can be a truly disastrous choice, especially if the data are to be used for molecular replacement. In addition, missing the largest terms degrades the continuity and information content of all electron-density maps derived therefrom. This point is relevant to several applications (Section 9.1.13).

(2) Reject only those pixels that are saturated, and fit average standard profiles estimated from the non-saturated spots. This gives a poorer estimate than if the pixels were not saturated, but for applications such as molecular replacement or direct methods where the high-intensity data are essential, it is certainly better than option (1).

(3) Reduce the exposure time to ensure that there are no overloaded pixels. This is a trade-off, because if there is a large contrast between the intensity of the weakest and the strongest terms in the pattern, then the weaker terms will have a low and possibly unacceptable signal-to-noise ratio under this regime.



references